



Experimental Anisotropy Results in Alberta Shales

Darrel Hemsing*

Institute for Geophysical Research, Edmonton, Alberta, Canada
dhemsing@phys.ualberta.ca

and

Douglas Schmitt

Institute for Geophysical Research, Edmonton, Alberta, Canada

Abstract

Introduction

Seismic anisotropy is the variation of wave speed through different directions in a material. Preferential mineral alignment, layering, and fracturing all cause this seismic anisotropy to be observed in many crustal rocks. Shale, in particular, exhibits a relatively large degree of anisotropy. Taking anisotropy into account will improve the quality of seismic images, helping to correctly locate 3-D targets and avoid potentially costly mispositions. Our laboratory is performing tests on shale cores from the WCSB to determine their velocities, elastic constants, and their relation to preferential mineral alignment. Here we focus on the technical details of the laboratory system used to measure P- and S-wave velocities in Alberta shale as well as some preliminary results.

Sample description and preparation

Shale samples were obtained from sites in the WCSB. Three small 2.54 cm diameter cores were cut perpendicular, parallel, and 45° to the bedding plane in each sample. The ends of each core were ground parallel to better than 0.1 mm. Accurate porosities will be obtained using both a Micromeritics™ Mercury Porosimeter, and a Micromeritics™ GeoPycnometer. The samples will also be further characterized using thin sections, X-ray diffraction, and scanning electron microscopy.

Experimental configuration and technique

An ultrasonic pulse transmission technique was used to determine the P- and S-wave velocities in the samples. The method consists primarily of a pressure vessel and a data acquisition system. A pulse generator provides a signal to piezoelectric (PZT) transducers attached to the sample inside the pressure vessel. The resulting wave is transmitted through the sample and recorded in 10 ns steps by an oscilloscope. The piezoelectric transducers generate compressional and shear waves with a frequency centered around 1 MHz. The signal is analyzed and the sample transit time is chosen at the first extremum. The sample velocity is then the sample length by the transit time. Figure 1 shows a typical set of S-wave traces. It is clear that the first arrival is earlier at higher pressures, indicating a higher velocity.

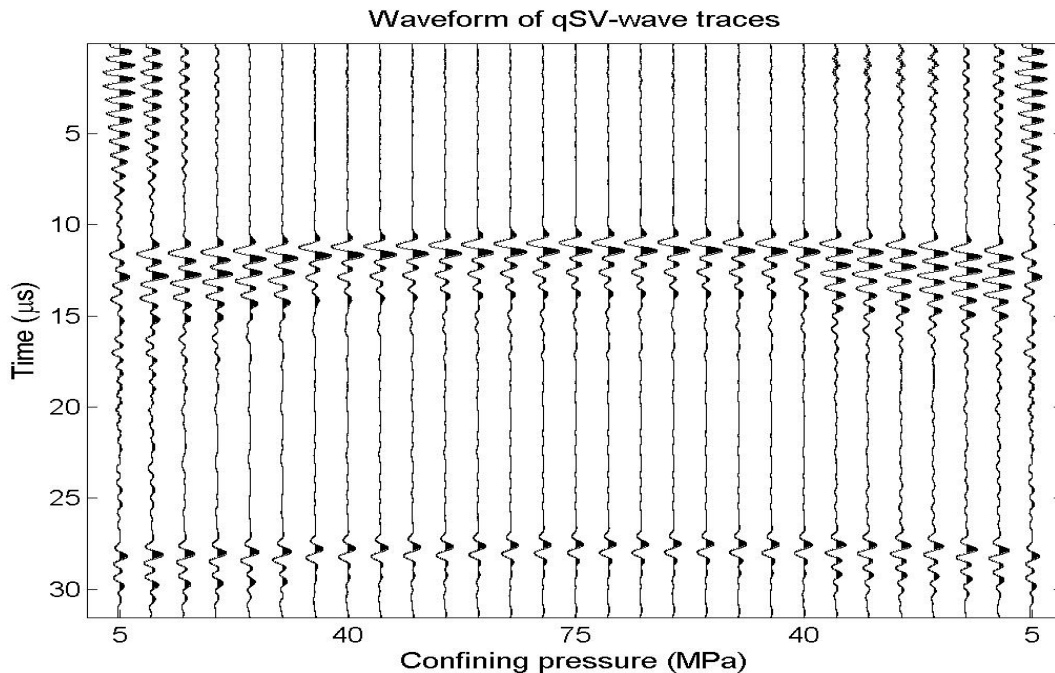


Figure 1. Traces of a typical S-wave. The first arrival indicated the transit time through the sample. For higher pressure, the first arrival is earlier than at low pressures. There is also a parasitic P-wave visible at the lower pressures. A reflection is also visible in each trace.

The pressure vessel being used is capable of producing pressures up to 200 MPa, in steps as small as 0.25 MPa using a hand driven pump. In practice, the samples are brought up to approximately in situ pressure, which varies from sample to sample. The transducers used in this experiment were created by stacking a P-wave PZT crystal on top of an S-wave PZT crystal (Fig 2a). This method allowed for larger crystals to be used, aiding in the strength of the signal. A backing of epoxy and iron, used to damp the signal, was set on the ceramics which were then placed onto aluminum buffers. To prevent leakage of the hydraulic oil confining fluid, the sample was placed into a PVC jacket (Fig 2b). Under the assumption of transverse isotropy for shales (e.g. Johnston & Christensen, 1995) the 5 necessary directions for determining elastic constants were measured, as well as one extra S-wave on the 45° core (Fig 3).

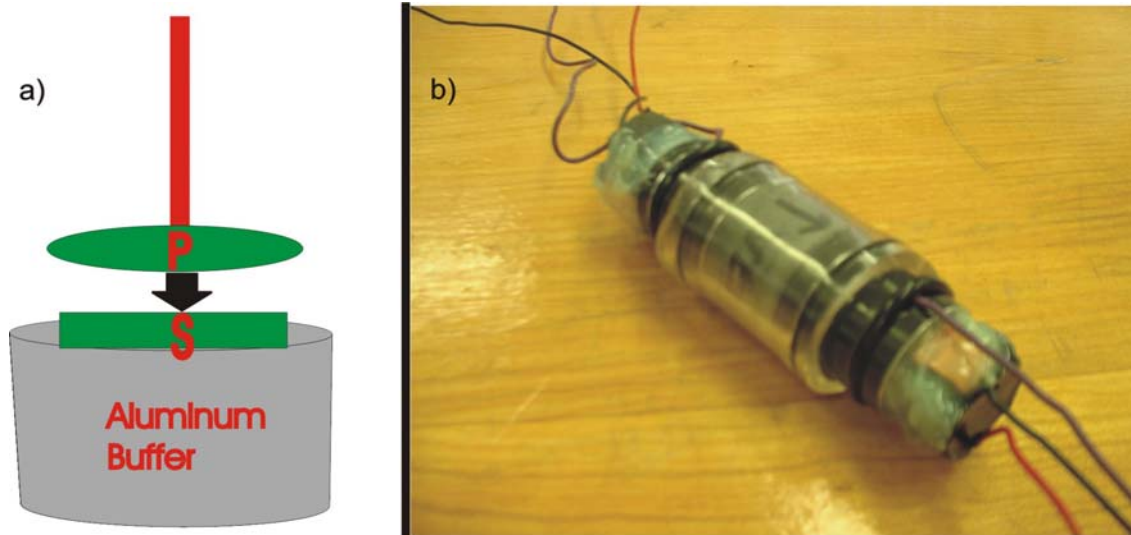


Figure 2. a) The P-wave crystal is stacked on top of the S-wave crystal, allowing for a higher energy transducer.
 b) A picture of the prepared sample. The sample is encased in PVC tubing with the transducers affixed to both ends.

S-wave propagation and polarization direction

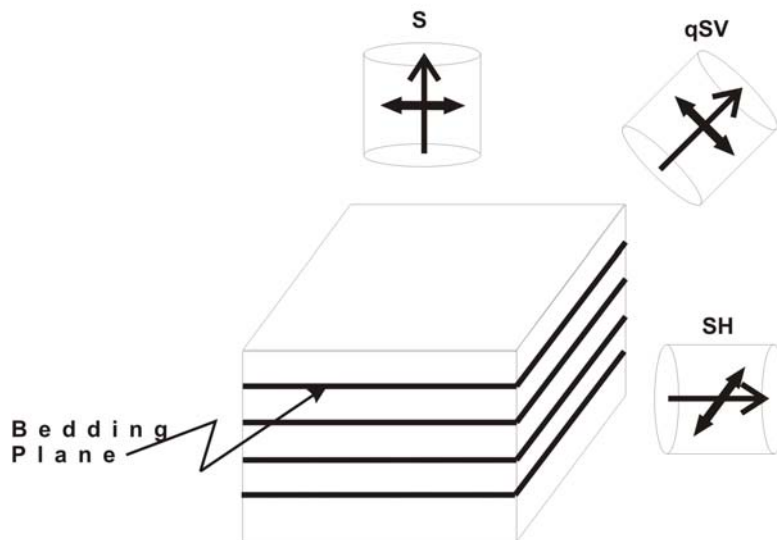


Figure 3. The direction of S-wave polarization in each of the cores. Cores were cut perpendicular, parallel, and 45° to the bedding plane. The perpendicular S-wave and the parallel SH-wave are necessary for derivation of elastic constants of TI material. P-waves were measured on all cores.

Experimental results

The velocity versus pressure curve for sample SSA-010 is shown in Figure 4. The velocities increase with pressure partly because of closing microcracks and increased grain contact. The anisotropy is also clearly evident. The anisotropies at select pressures are shown in Table 1. Although the velocities increase with increasing pressure, both the P- and S-wave anisotropies



decrease with increasing pressure. As the pressure is decreased, the anisotropies slowly start to increase again. There is a delay that is perhaps caused by microcracks opening at a lower rate than which they closed.

Table 1. Anisotropies for SSA-010 at selected increasing and decreasing pressures

Pressure (MPa)	P-wave anisotropy %	S-wave anisotropy %
20.0	17.5	10.0
40.0	15.8	10.5
75.0	13.9	9.8
40.0	13.5	10.1
20.0	15.1	10.5

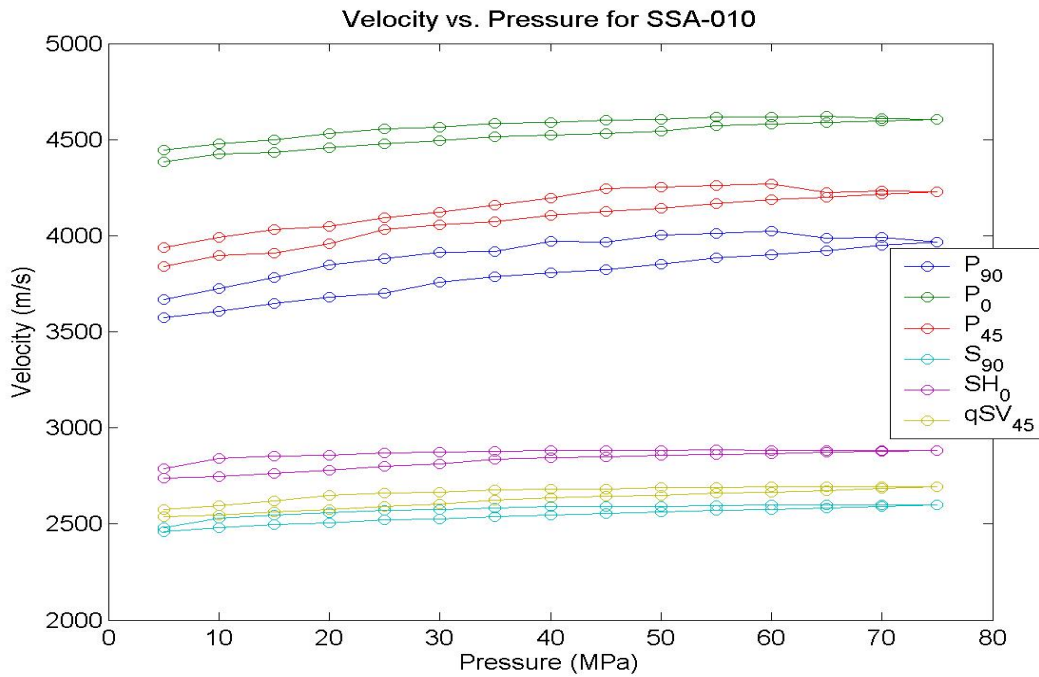


Figure 4. Velocity versus pressure curves for sample SSA-010. The sample is clearly anisotropic.

Figure 5 shows the elastic constants and anisotropic parameters ϵ , γ , and δ . The data shown here was calculated using an inexact density. The volume of the sample was calculated as a perfect cylinder. This however, does not take into account minor chips that may be present in the sample. A more accurate density will be obtained in the near future. The elastic constants all increase with pressure, while both epsilon and gamma decrease slightly with pressure.

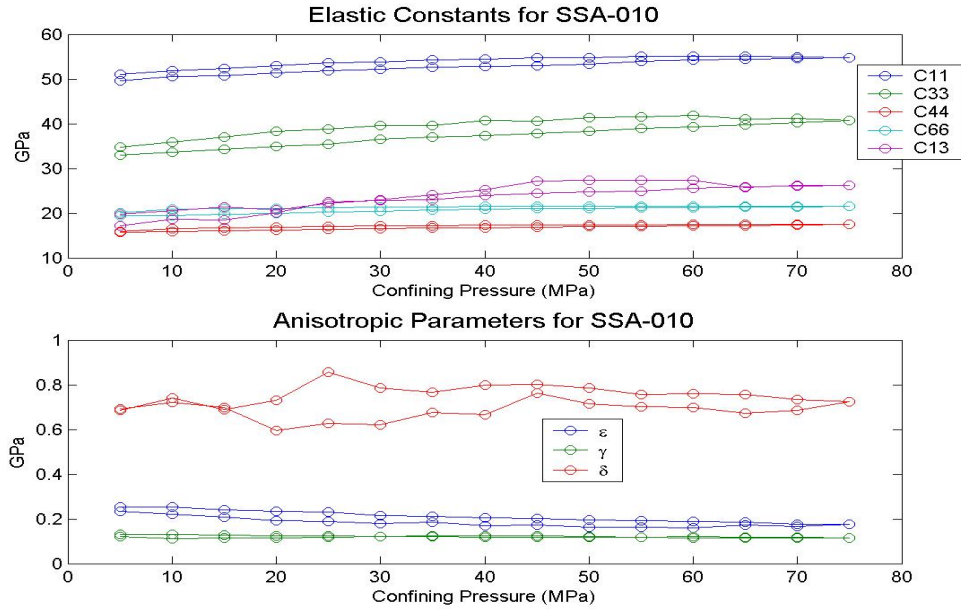


Figure 5. a) Elastic constants and b) anisotropic parameters for sample SSA-010. These values may be slightly inaccurate as a more precise density needs to be determined.

Conclusions

This preliminary data indicates a clear dependence of velocity and anisotropy on pressure. At higher pressures the velocity increases and the anisotropy decreases. Future work includes thin sections, X-ray diffraction, and SEM. This will help further classify the samples.

References

Johnston, J. E., and Christensen, N. I., 1995, Seismic anisotropy of shales: J. Geophys. Res., **100**, 5991-6003.